

To be submitted to  
Nuovo Cimento

ISTITUTO NAZIONALE DI FISICA NUCLEARE  
Laboratori Nazionali di Frascati

LNF-78/24(P)  
12 Giugno 1978

S. Bartalucci, G. Basini, S. Bertolucci, M. Fiori, P. Giromini,  
R. Laudan, E. Metz, C. Rippich and A. Sermoneta: EXPERI-  
MENTAL CONFIRMATION OF THE 1100 STRUCTURE AND  
FIRST OBSERVATION OF THE LEPTONIC DECAY OF THE  
 $\rho'(1250)$ .

EXPERIMENTAL CONFIRMATION OF THE 1100 STRUCTURE AND  
FIRST OBSERVATION OF THE LEPTONIC DECAY OF THE  $\rho'(1250)$ .

S. Bartalucci, G. Basini<sup>(x)</sup>, S. Bertolucci, M. Fiori<sup>(o)</sup>, P. Giromini,  
R. Laudan, E. Metz, C. Rippich and A. Sermoneta.

Deutsches Elektronen-Synchrotron DESY, Hamburg (Germany), and  
Laboratori Nazionali di Frascati dell'INFN, Frascati (Italy).

SUMMARY. -

We have extended our survey of the reaction  $\gamma + p \rightarrow p + e^+ + e^-$  by collecting 20000 additional  $e^+e^-$  pairs in the invariant mass region  $900 < m < 1500$  MeV. The measured interference pattern shows two enhancements at mass values of 1097 and 1266 MeV. The parameters of those structures, when interpreted as vector mesons in the VDM framework, are given.

XXXXXXXXXXXXXX

We measured the interference pattern in the  $e^+e^-$  final state of the Bethe-Heitler amplitude with the real part of the Compton diffractive photoproduction amplitude off hydrogen by studying the reaction

$$\gamma + p \rightarrow p + e^+ + e^- \quad (1)$$

---

(x) - Also at Laboratorio di Cosmogeofisica del CNR, Torino.

(o) - deceased.

The four diagrams contributing to the reaction (1) are shown in Fig. 1.

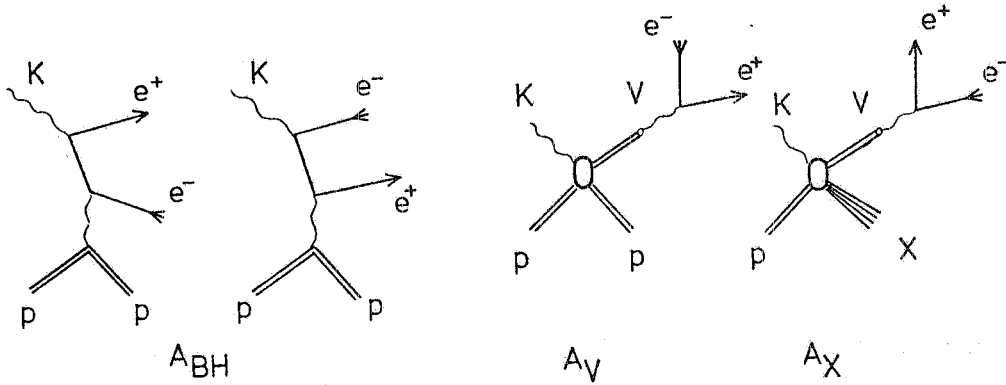


FIG. 1 - Feynman diagrams for reaction (1).

The Bethe-Heitler diagrams are calculated<sup>(1)</sup>, while the Compton amplitude is parametrized, according to the VDM, as

$$\sum_V A_V \propto \sum_V \frac{m_V^2}{m^2} \frac{ie^{i\varphi_V}}{m_V^2 - m^2 - im_V \Gamma_V} \sqrt{\frac{d\sigma_V}{dt} \frac{\Gamma_V}{m_V}} \quad (2)$$

using the notation

$$\frac{d\sigma_V}{dt} = \frac{d\sigma}{dt} (\gamma p \rightarrow p V (V \rightarrow e^+ e^-)) = \frac{d\sigma_V}{dt} (\gamma p \rightarrow V p) \Big|_{t=0} e^{b_V t} \text{BR}_{e^+ e^-} \quad (2)$$

Here  $m_V$  is the mass of the vector meson,  $\Gamma_V$  its width,  $\text{tg}(-\varphi_V)$  is the ratio of the real to imaginary part of the diffractive amplitude, and  $b_V$  its slope.  $m$  and  $t$  are the  $e^+e^-$  invariant mass and momentum transfer, respectively.

It follows from the charge-conjugation invariance principle that studying the asymmetry distribution of the experimental events as a function of kinematical variables which are antisymmetric in the four-momenta  $p_+$  and  $p_-$  of the lepton pairs, allows the measurement of the interference term between the Bethe-Heitler and the Compton amplitude. When the Compton production is appreciably smaller than the BH rate, we showed<sup>(3)</sup> that the search for new vector mesons is made with more sensitivity by looking at the interference term as a function of mass rather than by measuring the invariant mass spectrum.

More details about the theoretical background, the apparatus, and the experimental procedure can be found in refs. (3, 4). In this paper, we interpret the interference pattern produced by our publis

hed data<sup>(3)</sup> (19500  $e^+e^-$  pairs collected at three spectrometer angular settings of  $13^\circ$ ,  $15^\circ$  and  $16^\circ$ ) in combination with a new set of data (20000  $e^+e^-$  pairs recently collected at  $13^\circ$ ).

In particular we would like to mention that the new data differ from the previous ones at  $13^\circ$  by restricting the vertical dimensions of our  $\gamma$  beam by almost a factor two. In this way we improved our mass resolution (which is, apart from multiple scattering, directly proportional to the beam width<sup>(3)</sup>), and, by decreasing at the same time the background level, we reduced the probability of misidentifying good trajectories because of noise.

The measured mass yield of all these data has already been published<sup>(3,4)</sup>. The experimental interference yields are shown in Figs. 2 and 3. The interference pattern of the sum of the data collected at  $13^\circ$ , as well as the overall sum of our data, taken at all the angular settings, now show definite evidence for at least two resonance-like structures<sup>(3)</sup> following the  $\phi$  meson, at around 1100 MeV and 1260 MeV. The enhancement at 1260 MeV will be shown to be consistent with the expected  $\rho'(1250)$ . In Fig. 4 we present our data after removal of the apparatus acceptance. Plotted is the real part of the Compton amplitude  $A(\gamma p \rightarrow p \gamma_{\text{virtual}}) = |A| (-i) e^{i\delta}$  with a normalization such that  $\text{Re}(A) = \sqrt{\frac{d\sigma}{dt}} (\gamma p \rightarrow p \gamma_{\text{virtual}}) \sin \delta$ . It should be noted that, in the vicinity of a narrow resonance,  $\delta$  is a rapidly varying function of the  $e^+e^-$  mass; Fig. 4 shows  $\text{Re}(A)$  as average values over 20 MeV wide bins. These data show an additional, much broader structure rising from masses above 1350 MeV. It will be the object of future analysis, since the data taking in this mass range is still in progress. The present study is devoted only to the analysis of the 1100 and  $\rho'(1250)$  structures.

### Results on the $\rho'(1250)$ .

We fitted for  $m_{\rho'}$ ,  $\Gamma_{\rho'}$ ,  $d\sigma_{\rho'}/dt$  and  $\varphi_{\rho'}$  in the mass region  $960 < m < 1400$ . The slope  $b_{\rho'}$  was assumed to be  $6 \text{ GeV}^{-2}$ , which is typical for photoproduction of vector mesons - this value was shown<sup>(3)</sup> to be consistent with our data. The mass region from 1040 to 1140 was omitted from the fit in order to reduce the dependence of the fit results on the 1100 parameters. The  $\rho + \omega + \phi$  contributions have been calculated according to the best fit parameter values of ref. (4). Tail contributions under the  $\rho'$  coming from the higher mass structure have been calculated by simultaneously fitting the data also to a fictitious resonance above 1300 MeV with the standard four parameters ( $m$ ,  $\Gamma$ ,  $d\sigma/dt$ , and  $\varphi$ ). In this way we do not properly describe our data above 1400 MeV, but we found this procedure accurate enough to estimate the background under the  $\rho'$ . Strong correlations are found in the fit between the parameters of the  $\rho'$  and of the back-

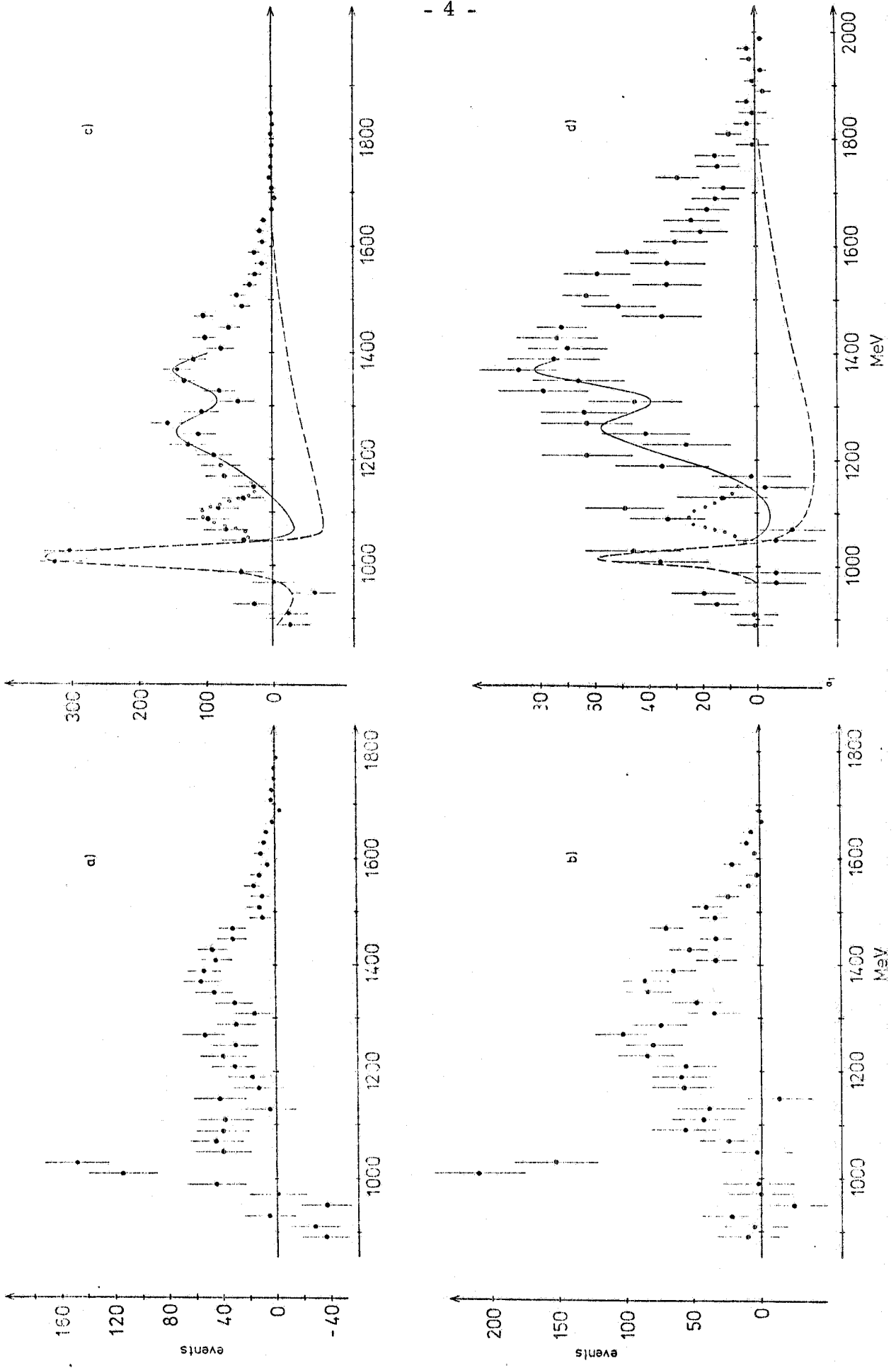
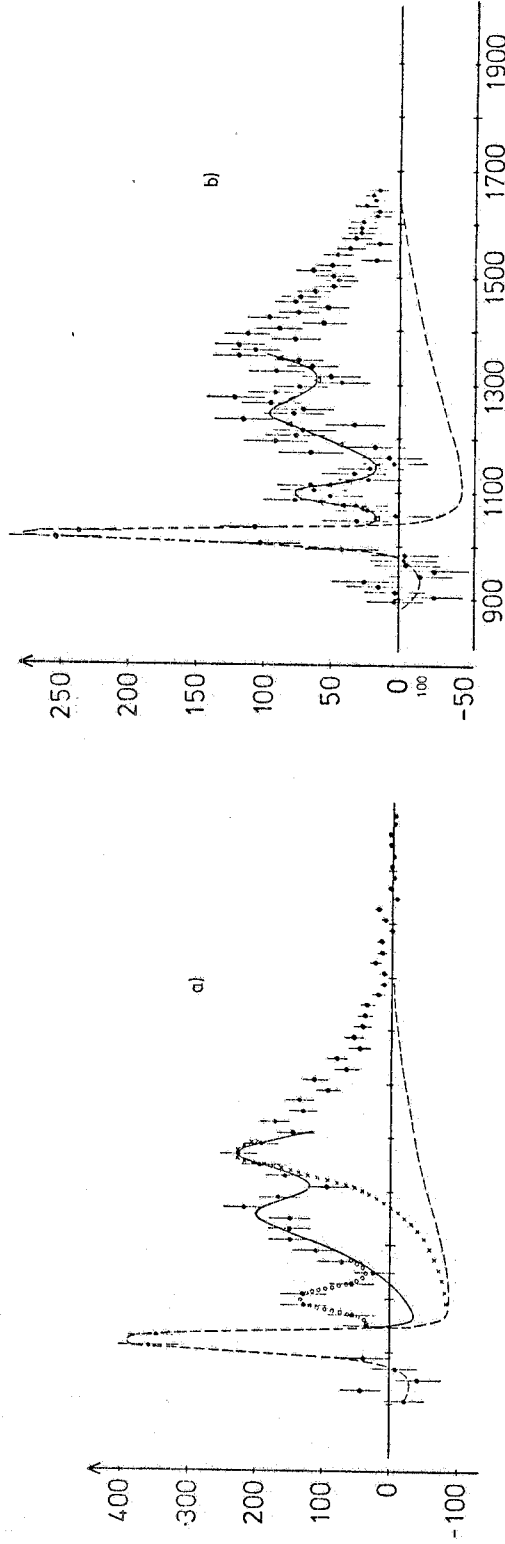


FIG. 2

**FIG. 2** - Spectrum of the interference events. Points with error bars are the experimental data. The dashed line represents the  $\rho + \omega + \phi$  contribution calculated according to the parameter values given in ref. (3). The solid line represents the calculated contribution of the  $\rho'$  and the higher mass fictitious structure. The values  $m_{\rho'} = 1266$  MeV,  $\Gamma_{\rho'} = 110$  MeV,  $\varphi_{\rho'} = 28^\circ$ ,  $d\sigma/dt(\gamma p \rightarrow p \rho'(\rho' \rightarrow e^+e^-)) = 41$  pb  $\text{GeV}^{-2}$  have been used. The circles represent the 1100 contribution, using  $m = 1097$  MeV,  $\Gamma = 31$  MeV,  $\varphi = 4^\circ$ ,  $d\sigma/dt_{t=0}(\gamma p \rightarrow p 1100(1100 \rightarrow e^+e^-)) = 14$  pb  $\text{GeV}^{-2}$ .

a) Old data collected with beam top energy  $K_{\text{max}} = 7.2$  GeV, central spectrometer momentum  $p_0 = 2700$  MeV, and spectrometer opening angle  $\theta = 13^\circ$ . b) New data collected at  $\theta = 13^\circ$ ,  $K_{\text{max}} = 7.2$  GeV,  $p_0 = 2700$  MeV. c) Sum of all the data collected at  $\theta = 13^\circ$ ,  $K_{\text{max}} = 7.2$  GeV,  $p_0 = 2700$  MeV. d) Old data collected at  $\theta = 15^\circ$  and  $16^\circ$ ,  $K_{\text{max}} = 7.2$  GeV,  $p_0 = 2700$  MeV.



**FIG. 3** - Interference spectrum of the sum of all the measured events at  $13^\circ$ ,  $15^\circ$ , and  $16^\circ$ . a) plotted in 20 MeV bins; b) plotted in 10 MeV bins. ----  $\rho + \omega + \phi$  contribution calculated according to ref. (4); — superimposed contribution of the  $\rho'$  and of the higher mass structure as from our best fit; \* \* \* \* background contributions under the  $\rho'$  from the higher mass structure as from our best fit; o o o o 1100 contribution; \* \* \* \* overall sum of all the contributions.

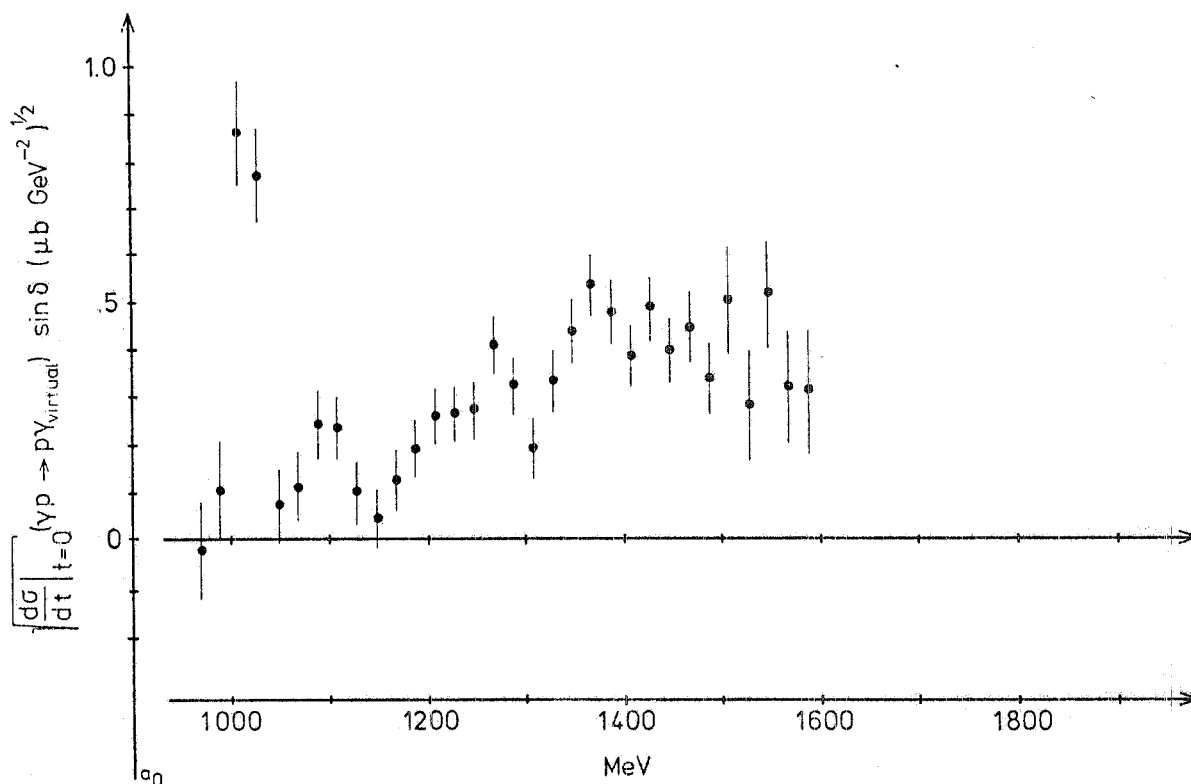


FIG. 4 - Real part of the virtual Compton amplitude as measured by the sum of our data at the three different angular settings (see text). In order to make comparisons with theoretical predictions one should keep in mind that the energy of the incoming photon producing a given virtual photon mass is dictated by our apparatus acceptance to be proportional to the spectrometer opening angle.

ground. Therefore, the errors, attached to the  $q'$ -parameter values (see Table I) are derived from a detailed study of the  $\chi^2$  contours and are defined by  $\chi^2 = \chi^2_{\text{min}} + 1$ .

TABLE I - Fitted parameters for  $q'^{(x)}$

|                   |   |   |
|-------------------|---|---|
| $M_{q'}$          | $1266 \pm 5 \text{ MeV}$  | $\frac{\chi^2}{\text{NDF}} = \frac{34.5}{43}$ |
| $\Gamma_{q'}$     | $110 \pm 35 \text{ MeV}$  |   |
| $d\sigma_{q'}/dt$ | $41 \begin{matrix} + 24 \\ - 19 \end{matrix} \text{ pb GeV}^{-2}$ |   |
| $\varphi_{q'}$    | $28^\circ \pm 8^\circ$  |   |

(x) - The quoted errors include systematic effects due to the background parametrization.

For any parametrization of the tail of the structure at masses above the  $\rho'$ , however, the statistical significance of the  $\rho'(1250)$  is always found to be at least a 5 s. d. effect. In particular, the best fit result gives  $m_{\rho'} = 1266 \pm 5$  MeV,  $\Gamma_{\rho'} = 110 \pm 20$  MeV,  $d\sigma/dt = 41 \pm 17$  pb GeV<sup>-2</sup>, and  $\varphi_{\rho'} = 28^\circ \pm 4^\circ$ .

In addition, for any combination of the  $\rho'$  - and the background-parameters inside the  $\chi^2_{\min} + 1$  contours plot, the overall resulting interference pattern changes by only a few percent at any mass value, even in the not fitted region around the 1100 MeV structure. Best fit results are shown in Figs. 2 and 3 and listed in Table I.

The  $\rho'$ , first daughter of the  $\rho$ -meson, is expected to appear at masses  $\simeq 1250$  MeV, to be  $\simeq 100$  MeV wide and to couple to the  $\underline{\text{photon}}$  with a strength indicated by  $\gamma_{\rho'}^2/4\pi = 8.3 \pm 3.1$ <sup>(5)</sup>.

Supporting, but not conclusive, experimental evidence for its existence was coming so far from the pion form factor, as measured at ACO and Novosibirsk<sup>(6)</sup>, which is well fitted by the ansatz of a  $\rho$ -pole plus a  $\rho'$  at 1.25 GeV, 150 MeV wide.

Frankiel et al.<sup>(7)</sup> have shown that a reasonable explanation, even if not unique, of their data from the  $p\bar{p} \rightarrow \omega\pi^+\pi^-$  annihilation was given by assuming the production, beside the B meson, of a  $J^P = 1^-$  state, decaying into  $\omega\pi$  with mass  $\simeq 1260$  MeV and width  $\simeq 120$  MeV. An  $\omega\pi$  enhancement, with  $J^P = 1^+$  or  $1^-$  and similar mass and width, has been also detected in several photoproduction experiments<sup>(8)</sup>. The measured photoproduction cross-section  $\sigma(\gamma p \rightarrow pV \text{ (} V \rightarrow \omega\pi \text{)}) \simeq 1 \mu\text{b}$  is found to be almost energy independent, as expected for the photoproduction of a  $J^P = 1^-$  state through the usual diffraction mechanism. These experiments, however, cannot rule out an explanation in terms of a non resonant Deck-effect production or of a B meson diffractive production via an orbital momentum  $l = 1$  exchange (violating the Gribov-Morrisson rule).

On the other hand, our experiment also determines a structure with similar mass and width and, furthermore, its observation in the  $e^+e^-$  decay mode makes the assignement of the quantum numbers  $J^P = 1^-$  unambiguous, and any contamination by Deck-type effects is impossible.

As additional consistency-check of our result, one can consider the VDM relation

$$\frac{\gamma_{\rho'}^2}{4\pi} = \left( \frac{\frac{\alpha^2}{12} \frac{m_{\rho'}^2}{\Gamma_{\rho'}} \frac{\gamma_{\rho'}^2}{4\pi} \frac{d\sigma}{dt}(\gamma p \rightarrow p\rho') \Big|_{t=0} (1 + \text{tg}^2 \varphi_{\rho'})}{\frac{d\sigma_{\rho'}}{dt} (1 + \text{tg}^2 \varphi_{\rho'})} \right)^{1/2} \quad (3)$$



which is obtained assuming that the total  $\rho'$ - $p$ - and  $\rho$ - $p$ - cross-sections are equal according to quark model. Using the values of  $m_{\rho'}$ ,  $\Gamma_{\rho'}$ ,  $\varphi_{\rho'}$ ,  $\frac{d\sigma_{\rho'}}{dt}$  from our best fit,  $\frac{\gamma_{\rho'}^2}{4\pi} = 0.64^{(8)}$ ,  $\varphi_{\rho'} = 37.5^{\circ(4)}$ , and  $\left. \frac{d\sigma}{dt}(\gamma p \rightarrow p\rho) \right|_{t=0} = 131 \mu\text{b GeV}^{-2(4)}$ , we get from (3)  $\frac{\gamma_{\rho'}^2}{4\pi} = 9.1$ , in rather good agreement with theoretical predictions<sup>(5)</sup>. Using such a value of a  $\gamma_{\rho'}^2/4\pi$  our experiment measures also  $\sigma(\gamma p \rightarrow p\rho')$  to be about  $1.5 \mu\text{b}$ , again in excellent agreement with the previously measured values of the  $\rho'$ -photo-production cross-section into  $\omega\pi$ <sup>(8)</sup>.

Results for the 1100 MeV structure.

We fitted for the 1100 parameters  $m$ ,  $\Gamma$ ,  $d\sigma/dt$  and  $\varphi$  in the mass region  $1040 < m < 1140 \text{ MeV}$ ; the slope  $b$  was assumed to be  $6 \text{ GeV}^{-2(3)}$ . The  $\rho + \omega + \phi$  contributions were included in the fit as measured in ref. (4), and the  $\rho'$  contribution was given by the minimum  $\chi^2$  parameters found above.

Best fit results are listed in Table II and shown in Figs. 2 and 3. The asymmetry distributions of the experimental events, together with the predicted yields for the  $\phi$  region, the 1100 region, and two neighbouring mass regions, are shown in Fig. 5.

TABLE II - Fitted parameters for the 1100<sup>(x)</sup>

|                     |  |   |
|---------------------|--|---|
| M                   | 1097 $\begin{smallmatrix} + 16 \\ - 19 \end{smallmatrix}$ MeV                  | $\frac{\chi^2}{\text{NDF}} = \frac{11}{11}$ |
| $\Gamma$            | 31 $\begin{smallmatrix} + 24 \\ - 20 \end{smallmatrix}$ MeV                    |   |
| $d\sigma_{1100}/dt$ | 14 $\begin{smallmatrix} + 9 \\ - 3.8 \end{smallmatrix}$ pb $\text{GeV}^{-2}$   |   |
| $\varphi$           | $4^{\circ} \begin{smallmatrix} + 36^{\circ} \\ - 42^{\circ} \end{smallmatrix}$ |   |

(x) - Errors are statistical only.

Under the assumptions made in the fit for the  $\rho + \omega + \phi + \rho'(1250)$  and high masses contributions, the result for  $d\sigma_{1100}/dt$  shows that the evidence for the 1100 structure is a 7 s. d. effect. Even if the individual calculated contributions of each vector meson can be affected by systematic errors due to the chosen theoretical approach, one should not forget that their overall contribution in the mass region around the 1100 MeV structure ( $1040 < m < 1140$ ) is finally extrapolated by using a very

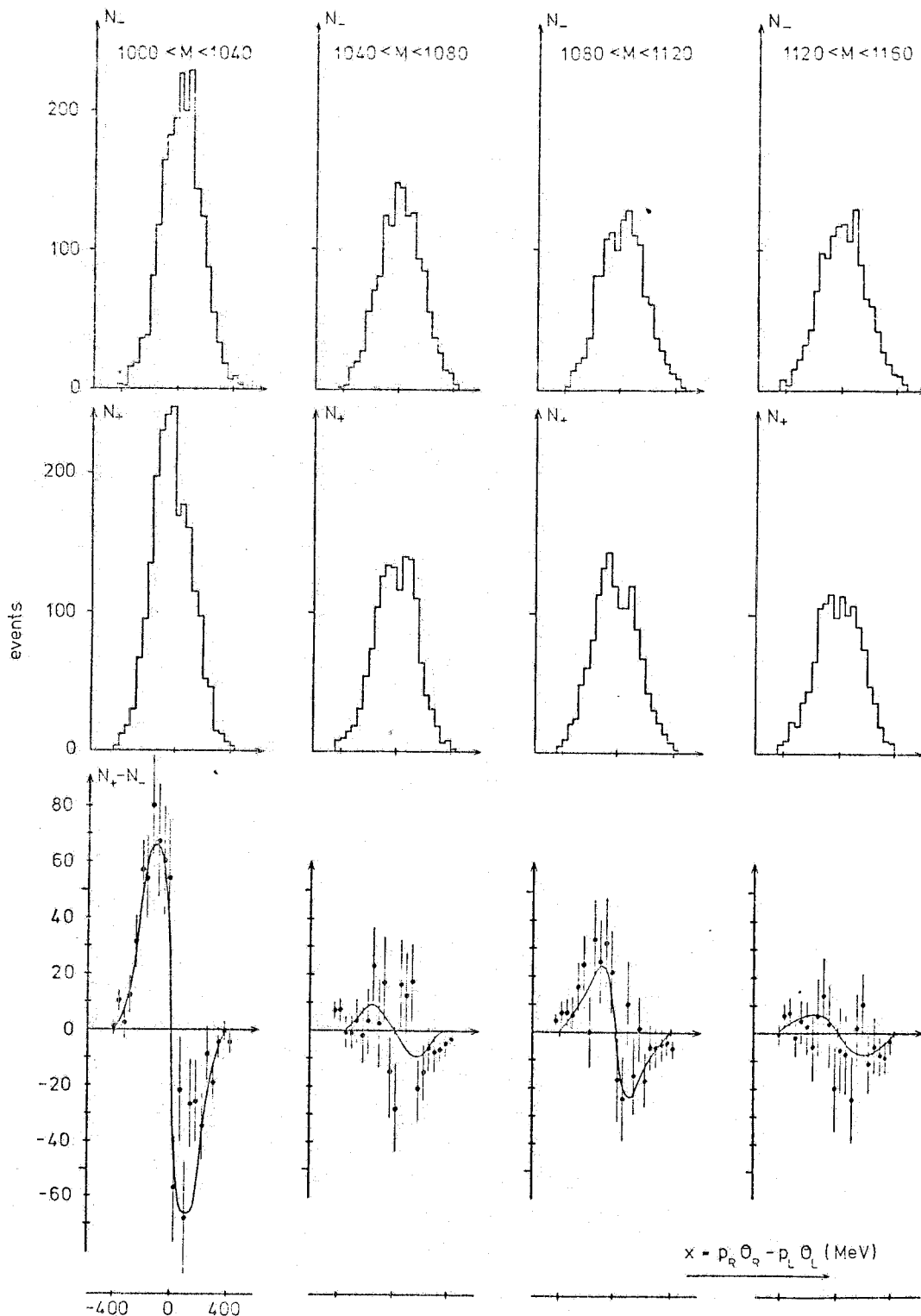


FIG. 5 - The measured asymmetry distribution as a function of  $x = p_R \theta_R - p_L \theta_L$  for each mass bin of 40 MeV from 1000 MeV to 1160 MeV.  $p_{L(R)}$  and  $\theta_{L(R)}$  are the momenta and the projected angles in the horizontal plane of the lepton going through the left (right) arm of the spectrometer.  $N^-$  denote the events collected when a positron or an electron is passing through the right arm of the spectrometer.

The integral  $\int (N^+ - N^-) \frac{x}{|x|} dx$  over a given mass bin measures the interference term in that particular bin. The predicted yields are calculated, using  $q + \omega + \phi$ , 1100 MeV,  $q'$ , and higher mass parameters from our best fits.

good fit ( $\chi^2/\text{NDF} = 34.5/43$ , see Table II) to the measured data in the mass range from 960 to 1400 MeV.

By inspection of equation (2) one can derive that the total strength of a Breit-Wigner resonance shows up in the interference spectrum proportional to  $\sqrt{d\sigma/dt(\gamma p \rightarrow Vp)BR_{e^+e^-}} \cos \varphi_V$ , whereas its contribution to the mass yield is proportional to  $1/\Gamma_V d\sigma/dt(\gamma p \rightarrow Vp)BR_{e^+e^-}$ . In our previous paper<sup>(3)</sup> we showed that the nonobservation of the 1100 in the mass yield<sup>(3, 4)</sup> is consistent with the signal measured in the interference pattern only if the width of such a state is larger than 5 MeV. With the now improved statistics, we determine the 1100 MeV width to  $31^{+24}_{-20}$  MeV, and the mass to  $1097^{+16}_{-19}$  MeV, using the interference data only.

### Conclusions.

We repeated our previous experiment<sup>(3)</sup> to study the reaction  $\gamma p \rightarrow pe^+e^-$ . The new collected data confirm the existence of a narrow structure at 1097 MeV. The improved statistics also indicate at 1266 MeV a structure 110 MeV wide, whose photoproduction parameters favour its identification with the long sought  $\rho'(1250)$ .

We are grateful for the support of the DESY Direktorium, who made this collaboration possible. The encouragement of Profs. P. Waloschek, G. Bellettini and I. Mannelli was of invaluable help. We thank F. Gutbrod, P. Söding and M. Greco for many interesting comments. We thank V. Chiarella, J. K. Bienlein for participation in parts of the runs, and D. Fong, C. Bradaschia and T. McCorrison who, in the past, largely contributed to the development of the data analysis programs we used in this experiment. We are grateful to Frl. U. Rehder, D. Habercorn, H. Lenzen, K. Löffler and M. Schneider for their skillful technical assistance. The warm cooperation of the Accelerator Group, of the Technical Support Groups, and of the Computer Center of DESY has been essential for the success of this experiment. A. S. thanks the Blaceflor Stieftelsen for financial support.

REFERENCES

- (1) - S. D. Drell and J. D. Walecka, *Ann. Phys.* 28, 18 (1964); M. L. Perl, T. Braunstein, F. Cox, F. Martin, W. T. Toner, B. D. Dieterle, T. F. Zip, W. L. Lakin and H. C. Bryant, *Phys. Rev. Letters* 23, 1191 (1969); B. Huld, *Phys. Rev.* 168, 1782 (1968); M. Damashek and F. Gilman, *Phys. Rev.* D1, 1319 (1970).
- (2) -  $BR_{e^+e^-} = \frac{\alpha^2}{12} \frac{4\pi}{\gamma_V^2} \frac{m_V}{\Gamma_V}$ , where  $\frac{\gamma_V^2}{4\pi}$  is the vector meson-photon coupling constant.
- (3) - S. Bartalucci, S. Bertolucci, M. Fiori, D. Fong, T. McCorrison, P. Giromini, S. Guiducci, C. Rippich, M. Rohde, A. Sermoneta and L. Trasatti, *Nuovo Cimento* 39A, 374 (1977).
- (4) - S. Bartalucci, S. Bertolucci, J. K. Bienlein, M. Fiori, P. Giromini, R. Laudan, E. Metz, C. Rippich and A. Sermoneta, *Nuovo Cimento* 44A, 587 (1978).
- (5) - A. Bramon, *Lett. Nuovo Cimento* 8, 659 (1973); G. Veneziano, *Nuovo Cimento* 57A, 190 (1968); A. Bramon and M. Greco, *Nuovo Cimento* 14A, 323 (1973).
- (6) - G. Cosme, A. Coureau, B. Dudelzak, B. Grelaud, B. Jean-Marie, S. Jullian, D. Lalanne, F. Laplanche, G. Parrour, R. Riscalla, Ph. Roy and G. Szklarz, *Orsay-LAL Report* 1287 (1976); V. M. Aulchenko, G. I. Budker, I. V. Vassermann, I. A. Koop, L. M. Kuradze, V. P. Kutovoy, A. P. Lisenko, S. I. Mishnev, E. V. Pakhtuseva, S. I. Sidorov, A. N. Skrinsky, G. M. Tumaikin, A. G. Khabkhashev, A. G. Chilingarov, Y. M. Shatunov, B. A. Schwartz, and S. I. Eidelman, *Tbilisi Conference Proceedings* (1976).
- (7) - F. Frenkiel, C. Ghesquiere, E. Lill est, S. V. Ching, J. Diaz, A. Ferrando and L. Montanet, *Nuclear Phys.* 47B, 61 (1972).
- (8) - J. Ballam, G. B. Chadwick, Y. Eisenberg, E. Kogan, K. C. Moffeit, I. O. Skillicorn, H. Spitzer, G. Wolf, H. H. Bingham, W. B. Fretter, W. J. Podolsky, M. S. Rabin, A. H. Rosenfeld, G. Smadja and P. Seyboth, *Nuclear Phys.* 76B, 375 (1974); K. C. Moffeit, *Proceedings of the Intern. Conf. on Electron and Photon Interactions at High Energies, Bonn* (1973), and reference therein.